# Nano-sized Cr-N cluster formation in Fe-35Ni-10Cr alloy during low-temperature plasma nitriding

Yulin Xie[1,*1], Goro Miyamoto[2,3] and Tadashi Furuhara[2]

[1]*Graduate School of engineering, Tohoku University, Katahira 2-1-1, Aoba-ku, Sendai 980-8577, Japan.*
[2]*Institute for Materials Research, Tohoku University, Katahira 2-1-1, Aoba-ku, Sendai 980-8577, Japan.*
[3]*Research Center for Structure Materials, National Institute for Materials Science (NIMS), Sengen 1-2-1, Tsukuba 305-0047, Japan.*

Expanded austenite ($\gamma_N$) formed by low temperature nitriding of austenitic stainless steel is a N-enriched fcc containing Cr-N short range ordering, but no direct observation of Cr-N clustering has been reported. In the present study, the nanostructure of an Fe-35Ni-10Cr (at%) alloy plasma-nitrided at 673K was investigated using transmission electron microscopy (TEM) and three-dimensional atom probe (3DAP) technique in this study. Nanosized Cr-N clusters were directly observed in the $\gamma_N$ accompanied with strong streaks in selected area diffraction, obvious modulated structure in TEM and Cr-N rich regions observed by 3DAP. Thermodynamic calculations suggested that Cr-N clusters were formed by spinodal decomposition due to a strong Cr-N attractive interaction. The hardness of the $\gamma_N$ layer was much higher than that of Fe-N austenite steel, which indicates that the hardness is not only due to nitrogen solid-solution hardening but also to a synergetic effect of the coexistence of Cr and N.

***Keywords:*** *Spinodal decomposition, austenitic steel, nitriding, three-dimensional atom probe (3DAP), expanded austenite.*

## 1. Introduction

The formation of a so-called expanded austenite ($\gamma_N$ or $\gamma_C$) layer on the surface of austenitic stainless steels during low temperature (~673K) nitriding has been widely investigated since the first studies in the 1980s[1,2)] showed the possibility of surface hardening without sacrificing the corrosion resistance of the material. The $\gamma_N$ produced by low-temperature nitriding of austenitic stainless steels with a Cr content of 18-20 at% is conventionally regarded as a nitrogen- supersaturated fcc solid solution with Cr-N short-range ordering[3)]. However, there is a significant possibility for $\gamma_N$ to be decomposed by nanoscale phase separation or spinodal decomposition due to the strong Cr-N attractive interaction[4)]. In the present study, Fe-35Ni-10Cr (at%) alloy was subjected to low-temperature plasma nitriding. Microstructures in $\gamma_N$ were revealed using transmission electron microscopy (TEM) and three-dimensional atom probe (3DAP).

## 2. Experiment

An Fe-35Ni-10Cr (at% as default, 9.21 wt% Cr) ternary alloy was cast by argon induction melting and hot working, while an Fe-35Ni base alloy was prepared by continuous casting and cold rolling. These alloys are denoted as the Base and 10Cr alloys, respectively. The alloys were homogenized and solution-treated at 1523 K to obtain a fcc single phase with no elemental segregation, and then cut into slices. The specimen surfaces were mechanically polished and then subjected to plasma-nitriding at 673 K for 30 h in a $N_2/H_2/Ar$ mixed atmosphere ($p(N_2)$: $p(H_2)$: $p(Ar)$=8: 4: 5) at a total pressure of 1000 Pa. After nitriding, the specimens were furnace-cooled to room temperature. After resin mounting, the specimens were mechanically polished and etched with a 2% Nital solution, and the cross-sectional microstructure was then observed using optical microscopy (OM) and field emission-scanning electron microscopy (FE-SEM; JEOL JSM-7001F, operated at 15 kV). Micro-Vickers hardness was tested at a load of 10 gf and the size of the indentations was measured using SEM. The N content was determined by field emission-electron probe microanalysis (FE-EPMA; JEOL JXA-8530F, operated at 15kV). Standard samples of pure iron and Fe-0.98, 2.0, and 5.9 mass% N ($Fe_4N$) were used for calibration. Nanostructures in the nitrided region were characterized using TEM (JEOL JSM2100-plus, operated at 200 kV) and 3DAP (CAMECA LEAP-4000HR). TEM and 3DAP samples were prepared using a focused ion beam (FIB; FEI Quanta 3D). 3DAP analysis was conducted at 50K with a pulse fraction of 20% and a pulse rate of 200 kHz. The data obtained from the 3DAP samples were analyzed using the IVAS ver. 3.8.8 software.

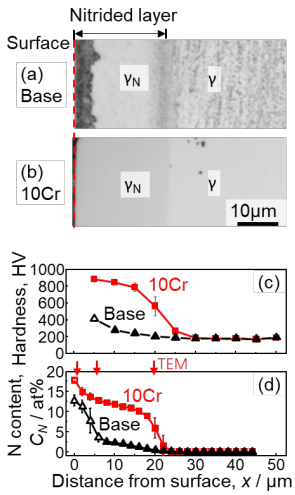


Fig. 1. (a,b) Optical micrographs, (c) hardness, and (d) N content-depth profiles for Base and Fe-35Ni-10Cr alloys nitrided at 673 K for 30 h. Arrows show the positions for TEM analysis of the 10Cr alloy in Fig. 2.

*1 Graduate Student, Tohoku University.

## 3. Results

Figs. 1(a) and 1(b) show cross-sectional OM images of the Base and 10Cr alloys nitrided at 673 K for 30 h, respectively. In Fig. 1(a), a diffusion layer ($\gamma_N$) with low contrast appears beneath the dark etched layer on the surface of the Base alloy, whereas the nitrided layer in the 10Cr alloy mostly consists of $\gamma_N$ with a thin dark layer on the surface (Fig. 1(b)). Figs. 1(c) and 1(d) show the hardness and N depth profiles for the nitrided alloys, where open symbols near the surface represent data taken from the dark layer. The $\gamma_N$ layer in the 10Cr alloy shows extremely high hardness (~900HV) and high N content (~15 at%) compared with the Base alloy (~300HV for the $\gamma_N$ layer, ~2.3 at% N). The N concentration and hardness gradually decrease towards the inner un-nitrided region for both alloys. The $\gamma_N$ layer is considered to be expanded austenite due to its high hardness, high N content and weak contrast after etching.

Fig. 2 shows selected area electron diffraction (SAED) patterns, bright field TEM images and intensity profiles taken from the SAED patterns for $\gamma_N$ in the 10Cr alloy nitrided at 673 K for 30 h at various depths from surface. At a depth of 0.5 μm (Fig. 2(a)), fcc spots with superlattice reflections indicate the presence of a $Fe_4N$ type ordered structure in $\gamma_N$, consistent with a previous report[3]. Modulation along $<010>_\gamma$, rather than precipitation, is observed in the bright-field TEM image. At a depth of 6.5 μm (Fig. 2(b)), $\gamma_N$ spots with no clear superlattice spots nor secondary phase were observed, but strong streaks along the $<001>_\gamma$ direction are present, and a clear modulated structure along $<010>_\gamma$, is observed in the bright-field TEM image. The vertical dashed lines in the intensity profiles represent the theoretical positions of CrN peaks, but no suck peaks are observed. Fig. 2(c) shows the results for the $\gamma_N$ layer at a depth of 20 μm from the surface, which is close to the growth front of $\gamma_N$. No superlattice reflections, streaks or modulation are observed, regardless of the high N content (5.9 at%) in this region; therefore, it is considered that $Fe_4N$ type ordering and modulation requires a certain N content[3] or time to evolve after N enrichment.

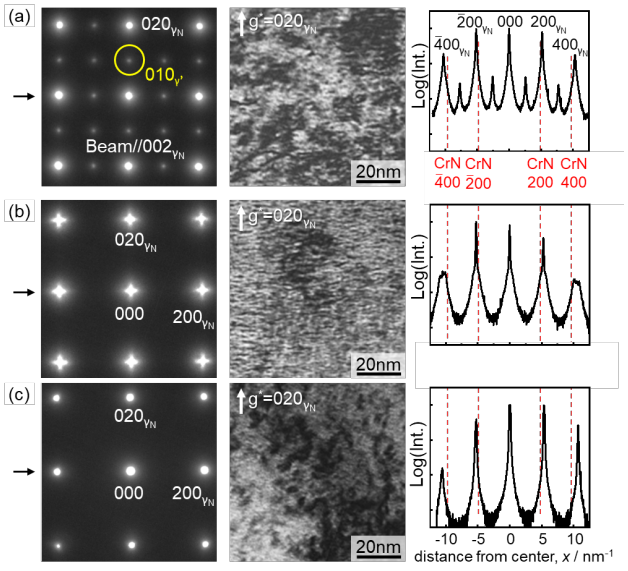


Fig. 2. SAED patterns, bright field images and intensity profiles taken from SAED patterns between $-400_{\gamma N}$ and $400_{\gamma N}$ for the nitrided 10Cr alloy, near the nitrided surface at a depth of (a) 0.5 μm, (b) 6.5 μm, and (c) 20 μm, respectively. The dashed lines show the peak positions for a standard CrN nitride (B1 type).

3DAP analyses were conducted to gain a deeper understanding of the chemical heterogeneity of $\gamma_N$ in the 10Cr alloy. Figs. 3(a) and 3(b) show Cr atom maps, where highlighted areas represent Cr-rich regions. The number density of Cr-rich regions at a depth of 4.5 μm is clearly higher than that in the un-nitrided region at a depth of 31.5 μm from the surface. Although the N content in Fig. 3(b) is considerably low (0.077 at%), isosurfaces are still observed due to the statistically higher local Cr composition in random distribution in the 3DAP data. The proxigram in Fig. 3(c) shows the concentration profile as a function of the distance from the isosurface shown in Fig. 4(a). Cr and N enrichment occurs simultaneously with a ratio close to 1:1, which indicates Cr-N clustering inside the $\gamma_N$ layer. Fig. 3(d) shows the variation in the N content obtained from 3DAP measurements at various depths from the surface, and these results are consistent with the FE-EMPA results for the N content shown in Fig. 1(d). The number density and the average volume of the Cr-enriched regions at each depth were quantified and the results are shown in

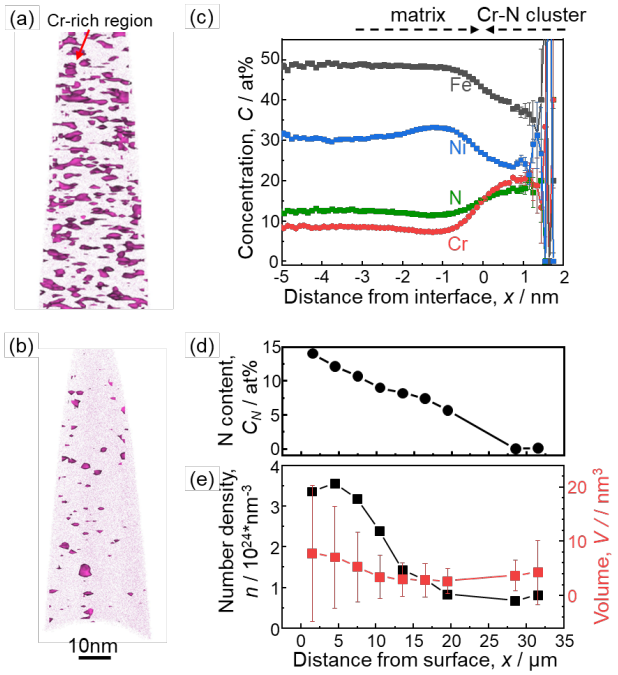


Fig. 3. 3DAP analyses of $\gamma_N$ in 10Cr alloy nitrided at 673 K for 30 h. Cr atom map at depths of (a) 4.5 μm ($\gamma_N$ layer), and (b) 31.5 μm (close to the growth front). (c) Proxigram revealing the concentration profile of each element across the isosurfaces of the data shown in (a). (d) Variations in N content for each 3DAP dataset with respect to the depth, and (e) variations in the number density and average volume of the Cr-enriched regions as a function of the depth from the surface. The highlighted isosurfaces in (a) and (b) represent regions where the local Cr content is 25% higher than the total Cr content.

Fig. 3(e). The region near the nitrided surface showed a higher number density and larger volume of clusters. These values then decreased with increasing depth or decreasing N content. Assuming spherical clusters, the average radius of the clusters was estimated to be 0.8-1.3 nm, as calculated from the volume data.

## 3. Discussion

Cr-N clustering was thus directly observed in this study using the 3DAP technique together with TEM/SAED analysis. The addition of Cr and N causes the free-energy surface to be upwardly convex due to the attractive Cr-N interactions, as schematically shown in Fig. 4(a). Therefore, it is possible for Cr-N clusters or nitrides to form by phase separation or spinodal decomposition in the fcc lattice. Figs. 4(b) and 4(c) show ternary diagrams of the (Fe-35Ni)-Cr-N system with binodal and spinodal lines calculated using Thermo-Calc2022a with the TCFE12 database. Based on the calculated binodal line, CrN nitride is expected to be produced with only a small addition of Cr and N through phase separation into fcc (Fe-35Ni) + B1-type nitride (CrN). Furthermore, the compositional range of $\gamma_N$ in this study falls into the spinodal region. The upper limit of the spinodal region is much lower than the composition of stoichiometric CrN; therefore, spinodal decomposition may lead to the formation of compositionally unstable Cr and N enriched fcc clusters, which is consistent with the lack of diffraction spots for CrN nitride in the SAED patterns shown in Fig. 2.

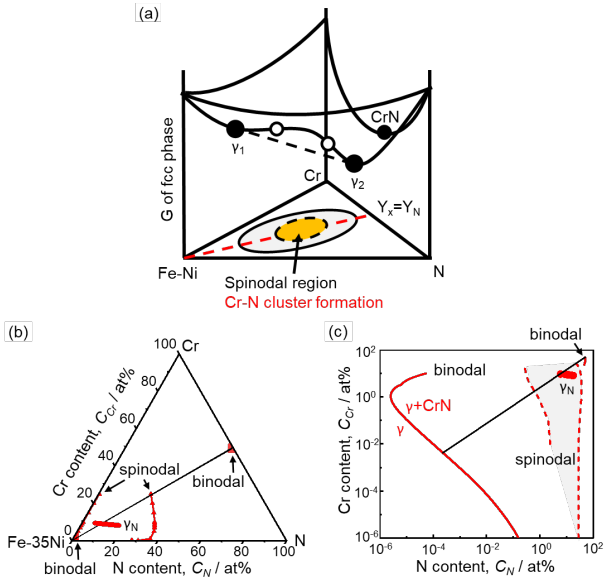


Fig. 4. (a) Schematic diagram of the free energy curved surface for (Fe-Ni)-Cr-N system. (b) ternary diagram of (Fe-35Ni)-Cr-N system showing binodal lines and spinodal lines. (c) same binodal lines and spinodal lines in (b) representing in log scale. The measured N content of $\gamma_N$ layer in this study is represented by the red line in (b) and (c), falling inside the spinodal decomposition region.

Studies on low-temperature nitriding of stainless steel to date have reported $\gamma_N$ layers with a hardness ranging from 400 to 1500 HV[5-8]. Compared with the hardness of Fe-N retained austenite, 283 HV for 8.6 at% obtained in this study and 280 HV for 10.0 at% N[9], the $\gamma_N$ layer in the 10Cr alloy was 600 HV harder with a similar N content. Apart from solution hardening, a large part of the high hardness observed in the $\gamma_N$ layers is due to the coexistence of Cr and N (Cr-N clusters or/and Cr-N SRO). Details of the hardening mechanism are a subject for further study.

## 4. Summary

In conclusion, Cr-N clustering in the expanded austenite layer formed during the low-temperature plasma nitriding of a Fe-35Ni-10Cr alloy was directly observed. Although a N solid solution appears to be present at the macroscopic level, nanostructural characterization of the $\gamma_N$ layer clearly showed the presence of Cr-N clusters, as evidenced by clear streaks in SAED patterns, a modulated structure in TEM images, and Cr/N-rich regions identified by 3DAP analyses. Thermodynamic calculations showed that the Cr-N clusters are formed by spinodal decomposition due to strong Cr-N attractive interactions. Compared with Fe-N retained austenite having a similar N content, the extremely high hardness of the expanded austenite is considered to originate from the synergetic effect of Cr and N. Nevertheless, there is a clear difference between the observed nanostructure of the 10Cr alloy in this study and that of stainless steel reported in the literature[3, 10-11]. Therefore, a similar characterization of commercial stainless steels is a necessary task for future study.


## Acknowledgments

This work was supported by JST SPRING, Grant No. JPMJSP2114, the JST "Collaborative Research Based on Industrial Demand" Grant No. JPMJSK1613, Japan and by the Tohoku University Microstructural Characterization Platform in Nanotechnology Platform Project sponsored by the Ministry of Education, Culture, Sports, Science and Technology (MEXT), Japan.


## References


1) Z. L. Zhang and T. Bell: Surf. Eng. 1 (1985) 131-136.
2) K. Ichii, K. Fujimura and T. Takase: Technol. Rep. Kansai Univ. 27 (1986) 135-144.
3) H. L. Che, S. Tong, K.S. Wang, M.K. Lei, M.A.J. Somers: Acta Mater. 177 (2019) 35-45.
4) T. Nishizawa, Thermodynamics of microstructure, (Japan Institute of Metals, Sendai, 2002), pp. 76-77.
5) C. Blawert, A. Weisheit, B. L. Mordike, and R. M. Knoop: Surf. Coat. Technol. 85 (1996) 15-27.
6) W. Liang, X. Xiaolei, X. Jiujun, S. Yaqin: Thin Solid Films 391(2001) 11-16.
7) A. Fossati, F. Borgioli, E. Galvanetto and T. Bacci: Surf. Coat. Tech. 200 (2006) 3511-3517.
8) E. Menthe, U.A. Bulak, J. Olfe, A. Zimmermann, K.-T. Rie: Surf. Coat. Tech. 133-134(2000) 259-263.
9) Y. Imai, M. Izumiyama, M. Tsuchiya: J. Japan Inst. Met. Mater. 29 (1965) 1047-1052.
10) M.K. Lei, X.M. Zhu: Biomaterials 22 (2001) 641-647.
11) J. C. Jiang and E. I. Meletis: J. Appl. Phys. 88 (2000) 4026-4031.